Journal of Advanced Research 40 (2022) 197–206

Contents lists available at ScienceDirect

Journal of Advanced Research

journal homepage: www.elsevier.com/locate/jare

Original Article

Fatty acid-binding protein 5 aggravates pulmonary artery fibrosis in pulmonary hypertension secondary to left heart disease via activating wnt/β-catenin pathway

Qian Lei [a], Zhimin Yu [a], Hang Li [a], Jun Cheng [a], Yanggan Wang [a,b,*]

[a] Department of Internal Medicine, Zhongnan Hospital of Wuhan University, Wuhan University, Wuhan, China
[b] Medical Research Institute of Wuhan University, Wuhan University, Wuhan, China

HIGHLIGHTS

- Bioinformatic analysis was performed to screen the key gene of PH-LHD.
- FABP5 was identified as a potential target for PH-LHD treatment.
- Inhibition of FABP5 improved cardiac function and mitigated pulmonary fibrosis in PH-LHD.
- FABP5 upregulated TGF-β1-mediated expression of pro-fibrotic proteins in PAFs.
- FABP5 regulated PAF activation partly via activating wnt/β-catenin pathway.

GRAPHICAL ABSTRACT

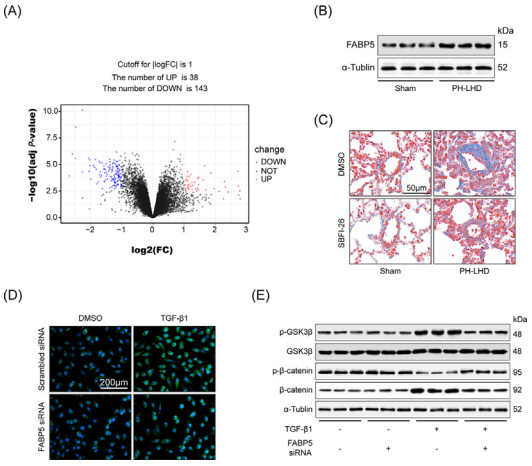

ARTICLE INFO

Article history:
Received 6 June 2020
Revised 1 October 2021
Accepted 21 November 2021
Available online 26 November 2021

Keywords:
FABP5
Wnt/β-catenin
Pulmonary artery fibrosis
Pulmonary hypertension
Pulmonary hypertension secondary to left heart disease

ABSTRACT

Introduction: Pulmonary hypertension secondary to left heart disease (PH-LHD) is a common and fatal disease. However, no effective therapeutic targets have been identified.
Objectives: Here, we set out to illustrate the functional role and underlying mechanisms of fatty acid-binding protein 5 (FABP5) in PH-LHD development.
Methods: We performed a systematic analysis of datasets GSE84704 and GSE16624 to identify differentially expressed genes and then constructed protein-protein interaction network for significant modules. Potential target genes in the modules were validated by RT-qPCR and western blot in a PH-LHD mouse model. PH-LHD or sham mice were treated with FABP5 antagonist SBFI-26 or DMSO for 28 days. The role of FABP5 on cardiac function was determined by echocardiography, its impact on pulmonary vascular remodelling were evaluated with right heart catheter, histological analysis and western blot. In vitro, primary pulmonary adventitial fibroblasts were used to investigate the pro-fibrotic mechanisms involving in FABP5.
Results: FABP5 was the only one dramatically upregulated along with increased protein expression in the established PH-LHD mouse model. Inhibition of FABP5 by SBFI-26 injection abrogated pulmonary artery

Peer review under responsibility of Cairo University.
* Corresponding author at: Department of Internal Medicine, Zhongnan Hospital of Wuhan University and Medical Research Institute of Wuhan University, Wuhan University, China.
E-mail address: wb000813@whu.edu.cn (Y. Wang).

https://doi.org/10.1016/j.jare.2021.11.011

remodelling in PH-LHD and improved cardiac function. In vitro, SBFI-26 or FABP5 siRNA blunted the TGF-β1-induced fibrotic response in cultured pulmonary adventitial fibroblasts. Mechanistically, FABP5 knockdown inhibited GSK3β phosphorylation and increased β-catenin phosphorylation. The wnt/β-catenin agonist SKL2001 diminished the antifibrotic effect of FABP5 knockdown on pulmonary adventitial fibroblasts under TGF-β1 stimulation.

Conclusion: FABP5 is an important mediator of pulmonary artery remodelling and a potential therapeutic target for PH-LHD.

Introduction

Pulmonary hypertension (PH) is a malignant pulmonary vasculopathy characterized by elevated pulmonary arterial pressure [1]. The persistently increased pulmonary artery pressure can ultimately lead to right heart dysfunction and subsequently death. Pulmonary hypertension secondary to left heart disease (PH-LHD), which was classified as group 2 PH by the World Health Organization, is the most common form of PH [2]. PH-LHD mainly occurs as a consequence of left heart failure, valvular heart disease (VHD), and left ventricular inflow or outflow obstruction [3]. Once PH-LHD has arisen, it not only worsens symptoms and exercise tolerance of heart disease, but also significantly increased morbidity and mortality [4]. However, due to insufficient understanding of pathological targets, the efficacy of anti-PH-LHD therapy is disappointing [5].

Fatty acid-binding protein 5 (FABP5), also termed epidermal fatty acid-binding protein (EFABP) or psoriasis-associated fatty acid-binding protein (PA-FABP), functions as a transporter of long-chain fatty acids (such as cannabinoid and retinoic acid) and some other ligands to assist intracellular localization, involving in fatty acid metabolism, inflammation, cell differentiation and proliferation [6]. FABP5 is widely expressed in many organs, such as epidermis, brain, lung, etc [7]. It has been reported that FABP5 plays vital roles in various diseases, such as type 2 diabetes and atherosclerosis [8,9]. FABP5 is also involved in the development of chronic obstructive pulmonary disease (COPD) and several types of cancers [10,11]. However, the role of FABP5 in the development of PH-LHD remains unclear.

Vascular remodeling in PH-LHD is characterized by pulmonary vascular adventitial thickening and stiffness. A pivotal change in the pulmonary vascular adventitia is the highly activated pulmonary adventitial fibroblasts (PAFs), which is featured by expression of α-smooth muscle actin (α-SMA) and secretion of a series of extracellular matrix such as fibronectin and collagen I, mainly stimulated by TGF-β1 [12,13]. It has been reported that FABP5 could activate human fibroblast WS1 cells via TGF-β1/SMAD2 pathway [14]. We assume that FABP5 may play a role in triggering PH-LHD through activating PAFs.

In this study, we performed bioinformatic analysis with two microarray datasets (GSE84704 and GSE16624) to identify potential key genes involving in the development of PH-LHD. Then, we established PH-LHD mouse model by ligating coronary left main artery (LMA) and validated the selected genes in the lungs using RT-qPCR and western blot. FABP5 was the only one that was upregulated in PH-LHD mice compared with sham mice. Next, we investigated the role of FABP5 in PH-LHD mice and found that, inhibition of FABP5 significantly improved cardiac function and attenuated pulmonary vascular remodeling and pulmonary artery fibrosis. Furthermore, we investigated the role of FABP5 in primary PAFs and found that both inhibition and knockdown of FABP5 could block PAFs activation. Mechanistic study suggested that the activation of wnt/β-catenin pathway contributes significantly to PAFs activation.

Materials and methods

Acquisition of microarray data

Two microarray datasets (GSE84704 and GSE16624) detailing the gene expression profiles of left heart disease-associated pulmonary hypertension were obtained from Gene Expression Omnibus (GEO) database (http://www.ncbi.nlm.nih.gov/geo/). Both GSE84704 and GSE16624 were performed on [Rat230_2] Affymetrix Rat Genome 230 2.0 Array (GPL1355 platform).

Data processing

A data meta-analysis was performed, including six lung samples from PH-LHD and six normal lung samples. The raw microarray data was subjected to background correction, quantile normalization, probe summarization, and base 2 logarithm conversions. Batch effect was removed by using the Affy package in R [15]. After obtaining the gene expression matrix, an unpaired *t*-test in the limma package (http://www.bioconductor.org/packages/release/bioc/html/limma.html) was applied to screen out differentially expressed genes (DEGs) [16]. DEGs were identified using a cut-off value of adj *P*-value < 0.05 and |logFC| > 1. Furthermore, hierarchical clustering analysis of DEGs was performed using pheatmap package in R (https://cran.r-project.org/web/packages/pheatmap/index.html).

Protein-protein interaction (PPI) network construction and modules selection

First, the probe ID for every DEG was converted to a gene symbol using a Perl script. If there were multiple probes for a particular gene, these were reduced. Then, the remaining DEGs were uploaded to the Search Tool for the Retrieval of Interacting Genes (STRING, https://string-db.org/) to construct PPI network [17]. The significant interactions were identified through extracting PPI pairs with combined score > 0.4 and visualized based on Cytoscape (http://www.cytoscape.org/) [18]. MCODE, a plugin to Cytoscape [19], was performed to detect modules of PPI network with the following cutoff threshold: degree cutoff = 2, k-core = 2, node score cutoff = 0.2 and maximum depth = 10012.

Mouse PH-LHD model

The PH-LHD model was induced in mice by ligation of left main artery (LMA). In brief, the mice were anesthetized with sodium pentobarbital (60 mg/kg; Merck, China) intraperitoneally and mechanically ventilated with the HX-101E small animal ventilator (Thaimeng Software, Chengdu, China). After exposure of the heart through a left thoracotomy at the 3rd–4th intercostal space, myocardial infarction (MI) was induced by ligating LMA using a 7-0 polyester suture. Successful coronary occlusion was confirmed by appearance of a pale area below the suture knot and ST segment elevation in the surface electrocardiogram (ECG) monitoring. Sham

animals underwent the same procedures except that the polyester suture was placed around the LMA without being tied.

Experimental design

Adult C57 mice (8–12 weeks old with weight of 18–25 g) were used to perform animal experiments. All animal studies were conducted in accordance with the Animal Care and Use Committee Guide of Wuhan University, which conforms to the Guide for the Care and Use of Laboratory Animals of the National Institutes of Health (NIH publication no. 85–23, revised 1996). Three separate experiments were performed:

Protocol 1

To identify potential target of PH-LHD, we first detected the expression of genes in the modules screened by bioinformatics. Mice were then randomly assigned to the sham or PH-LHD group. 28 days after operation, the establishment of PH-LHD model was validated by echocardiography and hemodynamic catheterization. After that, mice were euthanized with pentobarbital sodium (ip., 50 mg/kg). The chest was opened to exposure heart and lung. PBS at 4 °C was slowly injected from right ventricle until the pulmonary lobe became white. The lung and heart were quickly separated for histological and further analysis. The right ventricle and the left ventricle with septum were weighted individually to calculate the right ventricle hypertrophy index (RVHI). RVHI = the right ventricle weight/(left ventricle + septum weight). The expressions of potential critical genes of the modules in lung tissue were validated using RT-qPCR (n = 6 mice per group) and Western blot (n = 6 mice per group).

Protocol 2

To determine the effect of FABP5 on cardiac function and pulmonary vascular remodelling in PH-LHD, 46 surviving mice were divided into four groups: sham + DMSO (n = 6), sham + SBFI-26 (n = 6), PH-LHD + DMSO(n = 18) and PH-LHD + SBFI-26 (n = 16, SBFI-26 was used to inhibit FABP5). 100 mg SBFI-26 was dissolved in 1 ml DMSO and diluted 100 times with saline before use. SBFI-26 at a concentration of 2 mg/kg/d (i.p) [20] was given for 28 days from post-operation day 1. Saline with 1% DMSO was used as control. On day 28 after injection, the influence of FABP5 on left cardiac function was determined by ultrasound. Hemodynamic parameters were measured using a right heart catheter. The impacts of FABP5 on cardiac infarct size and pulmonary vascular fibrosis were assessed by histological analysis (n = 6 mice per group).

Protocol 3

For in vitro study, pulmonary adventitial fibroblasts (PAFs) were isolated from male C57BL/6 mice (n = 5). The procedures for cell isolation and culture are detailed in cell culture section. Cells were collected and fibroblast phenotype was confirmed by immunofluorescence. PAFs with/without FABP5 knockdown were incubated in serum-free Dulbecco's modified Eagle medium (DMEM) medium for 24 h, and subsequently stimulated with 10 ng/ml TGF-β1 in the absence of serum for another 24 h. To inhibit FABP5 activity, 100 μM of SBFI-26 (HY-117506B; MedChemExpress) was added at the beginning of TGF-β1 stimulation for 24 h. Similarly, the wnt/β-catenin pathway agonist SKL2001 (HY-101085, MedChemExpress), at a final concentration of 20 μM, was added at the beginning of TGF-β1 stimulation for 24 h. The expression of Col I, α-SMA and proteins involved in wnt/β-catenin pathway were detected using Western blot.

Echocardiography

Echocardiography was performed on 28 days after operation (n = 3–5 per group) using a VINNO 6VET High Resolution Ultrasonic Imaging System (VINNO, China). Left ventricular ejection fraction (EF) and fractional shortening (FS) were measured from at least three consecutive cardiac cycles and then averaged. Image analyses were then conducted by an observer blinded to the treatment of mice.

Cardiac hemodynamic

The mice were anesthetized with pentobarbital (50 mg/kg, Merck, China). The catheter (BD Biosciences, Franklin Lakes, NJ), filling with 12500U/L heparin sodium saline, was inserted into the right external jugular vein and then reach the right ventricle. All analyses were performed using the BL-420F information data acquisition and processing system. Right ventricle systolic pressure (RVSP) was calculated.

Total RNA isolation and RT-qPCR

Total RNA from lung tissues was extracted using TransZol Up Plus RNA Kit (transgene, ER501-01, China) following the manufacturer's instructions. 1 μg of total RNA was used to reverse transcribe to cDNA with the HiScript II Q RT SuperMix (Vazyme, R223-01, China). qRT-PCR analysis was carried out using the SYBR qPCR Master Mix (Vazyme, Q221-01, China) to detect the expression levels of target genes. All target genes were normalized to GAPDH (forward primer: ATGACATCAAGAAGGTGGTGAAG, reverse primer: CCTGTTGCTGTAGCCGTATTC). Data were collected and analysed using Bio-Rad CFX3.1 software (Bio-Rad, Maastricht, The Netherlands).

Western blot

Proteins were extracted using RIPA buffer (Beyotime, China) containing protease inhibitor (Complete Mini EDTA-free®, Roche) and phosphatase inhibitor (PhosSTOP, Roche) for western blot. The samples were then centrifuged at 12,000 rpm at 4 °C for10 min, and the supernatant was collected. The supernatant protein content was quantified using the BCA method (Beyotime, China). Equal amounts of protein were separated on SDS–polyacrylamide gels (10%) and electro-transferred to NC membranes. After being blocked by skim milk, the membranes were incubated with primary antibodies against FABP5 (1:1000, Proteintech, 12348-1-AP), IGF1 (1:500, Abconal, A11985), Col1 (1:500, Abcam, ab138492), α-SMA (1:1000, Ptoteintech, 14395-1-AP), GSK3β (1:2000, Proteintech, 22104-1-AP), p-GSK3β-Ser9 (1:1000, Proteintech, 67558-1-Ig), β-catenin (1:2000, Proteintech, 51067-2-AP), p-β-catenin-S33/S37/T41 (1:500, Abconal, AP0524) and α-Tubulin (1:1000, Proteintech, 11224-1-AP) at 4 °C overnight. The membranes were washed using TBS containing Tween-20, and then incubated with the respective HRP-conjugated secondary antibody (1:5000, Boster, BA1054/BA1050) for 1 h at room temperature. Blot reactions were developed using chemiluminescence solution and visualized with a ChemiDoc Touch Imaging System (Bio-Rad, USA). Specific bands were quantified under Image J software (National Institutes of Health, USA).

Histological analyses

28 days after operation, the heart and lung tissues were collected and washed with PBS at 4 °C. Samples were then fixed with 4% paraformaldehyde and undergone dehydration and paraffin embedding. Tissue slices (4 μm) were stained with hematoxylin

and eosin (HE) for structural evaluation and with Masson's trichrome staining for the assessment of pulmonary artery fibrosis. The slice images were captured using an Aperio VERSA System (Leica Biosystems, Germany) and analysis was carried out using the Image J software (National Institutes of Health, USA).

1) The ratio of infarcted area to the whole left ventricle was calculated to assess infarct size.
2) Pulmonary vascular remodelling was assessed by the percent of medial wall thickness (MT%) and percent of medial wall area (MA%) [21]. Pulmonary arteries with external diameter from 20 to 50 μm were measured to calculate MT% and MA% (ten vessels for each mouse). MT% = 100×(medial wall thickness)/(vessel semi-diameter), MA% = 100×(cross-sectional medial wall area)/(total cross-sectional vessel area).
3) Collagen deposition in pulmonary arteries was determined by calculating the percentage of blue-positive area over the total area of the image. A total of sixty vessels from six mice were analysed for each group (ten vessels per mouse).

Cell culture

The pulmonary artery was isolated, and the whole section was cut longitudinally and opened into a flat sheet. The aorta was isolated similarly. Fibroblasts were prepared using the technique described previously [22] with some modifications. Briefly, muscular tissue and endothelial cell layers were removed by gentle abrasion of the vessel. The remaining tissue was then dissected into 1-mm^3 portions and evenly distributed over the base of a 25-cm^2 culture flask containing 2 ml of DMEM with 20% FBS, supplemented with 1% penicillin and 1% streptomycin at 37 °C in 95%O_2 and 5% CO_2. After 5 days, fibroblasts were passaged and cultured in DMEM containing with 20% FBS. Afterwards, the isolated cells were detected by immunofluorescence using antibodies against vimentin. PAFs, which are positive for vimentin, accounted for >95%. The passage 3rd to 6th were used for the following experiments.

FABP5 siRNA transfection

Knockdown of FABP5 was conducted by transfecting siRNA. Briefly, before transfection, PAFs were dissociated and resuspended at a cellular density of 1×10^5/ml. Cell suspensions were transfected with siRNA at a final siRNA concentration of 10 nM specifically against FABP5 (sense, 5′AATGATACAGTCTGGCTTGGCTT3′; antisense, 5′GCCAAGCCAGACTGTATCATTTT3′) or scrambled siRNA (sense, 5′TCAAGCGTGCTAAGTATGGTCTT3′; antisense, 5′GACCATACTTAGCACGCTTGATT3′) using Lipofectamine 2000 (Invitrogen, Carlsbad, CA, USA) for 48 h. The efficiency of transfection was evaluated by western blot.

Immunofluorescence

The slices seeded with PAFs were fixed in paraformaldehyde for 30 min at room temperature. 0.5%Triton-X was used to penetrate the cells. To prevent nonspecific background staining, the slices were blocked by 5% BSA for 1 h. Then slices were incubated with primary antibody α-SMA (1:100, Proteintech, 14395-1-AP) overnight at 4 °C, followed by incubation with corresponding secondary antibody (1:1000, goat-anti-rabbit Alexa Fluor 488-conjugated antibody, Cell signaling technology) for 1 h at room temperature. The nuclei were stained with DAPI (1:2000, Sigma-Aldrich, USA) for 30 min at room temperature. The fluorescence was captured with a fluorescence microscope (Leica TCS-SP5II, Germany). Three images of each simple were used for quantification.

Statistical analysis

Statistical analysis was performed using GraphPad Prism 6 (GraphPad Software Inc, USA). All data were subjected to Sapiro-Wilk tests for normality. If data follow normal distribution, the unpaired *t*-test and ANOVA with Tukey's test correction were adopted, otherwise non-parametric test (Mann-Whitney test and Kruskal-Wallis with Dunn's test) was preferred. All data were presented as means ± SD. $P < 0.05$ was considered statistically significant.

Results

Bioinformatic screened key genes of PH-LHD

After integrated analysis of the mRNA expression profiles, a total of 181 DEGs were obtained in lung samples of PH-LHD. In comparison with normal lung samples, 38 DEGs were downregulated and 143 DEGs were upregulated (Fig. 1A). Hierarchical clustering analysis showed that the identified DEGs were significantly different in the two groups (Fig. 1B). The probe ID for every DEG was converted to a gene symbol using a Perl script. If there were multiple probes for a particular gene, these were reduced, and the entire group was treated as a single gene. The remaining 163 DEGs (including 36 down-regulated genes and 127 up-regulated genes) were uploaded to perform PPI analysis. The PPI network of DEGs consisted of 122 nodes and 494 edges (Fig. 1C). Five significant modules were obtained from PPI network of DEGs using MCODE (Fig. 1D-H).

FABP5 was identified as a potential target of PH-LHD

28 days after MI, the left ventricular wall of MI mice became thinner and dilated (Fig. 2A). Echocardiography revealed significant reduction of ejection fraction (EF) and fractional shortening (FS) (Fig. 2B-D). HE staining of lung tissue showed significantly increased MT% and MA% of pulmonary artery (Fig. 2E-G), the indicators for pulmonary vascular remodelling. In addition, the RVSP and right ventricular hypertrophy index (RVHI) were significantly increased in the MI mice (Fig. 2H-I), an indication of pulmonary hypertension. These data demonstrated successful establishment of the PH-LHD mouse model. Then, we examined the expression of the genes identified by above five modules in lung tissues from the sham and PH-LHD mice using RT-qPCR. The results showed that only FABP5 and IGF1 were significantly increased in lung tissue of PH-LHD mice (Fig. 2J). Next, we examined the protein expression of FABP5 and IGF1 in lung protein samples and found that FABP5, rather than IGF1, was significantly elevated in PH-LHD mice (Fig. 2K-N). Therefore, FABP5 was identified as a potential target for PH-LHD treatment.

FABP5 inhibition improved cardiac function and blunted pulmonary vascular remodeling

We next suppressed the activity of FABP5 in vivo using SBFI-26. We found that the infarct area was unaltered with SBFI-26 treatment (Fig. 3A, C). However, SBFI-26 significantly increased EF and FS as showing in Fig. 3B, D, E. MI-induced heart failure significantly increased MT% and MA%, whereas SBFI-26 significantly reduced the heart failure-induced increase of MT% and MA% (Fig. 3F, G, I). In addition, heart failure significantly increased the RVSP and RVHI respectively, whereas preventive administration of SBFI-26 significantly decreased the RVSP and RVHI (Fig. 3J, K). Masson's trichrome staining showed that SBFI-26 effectively prevented the development of pulmonary artery fibrosis (Fig. 3H, L).

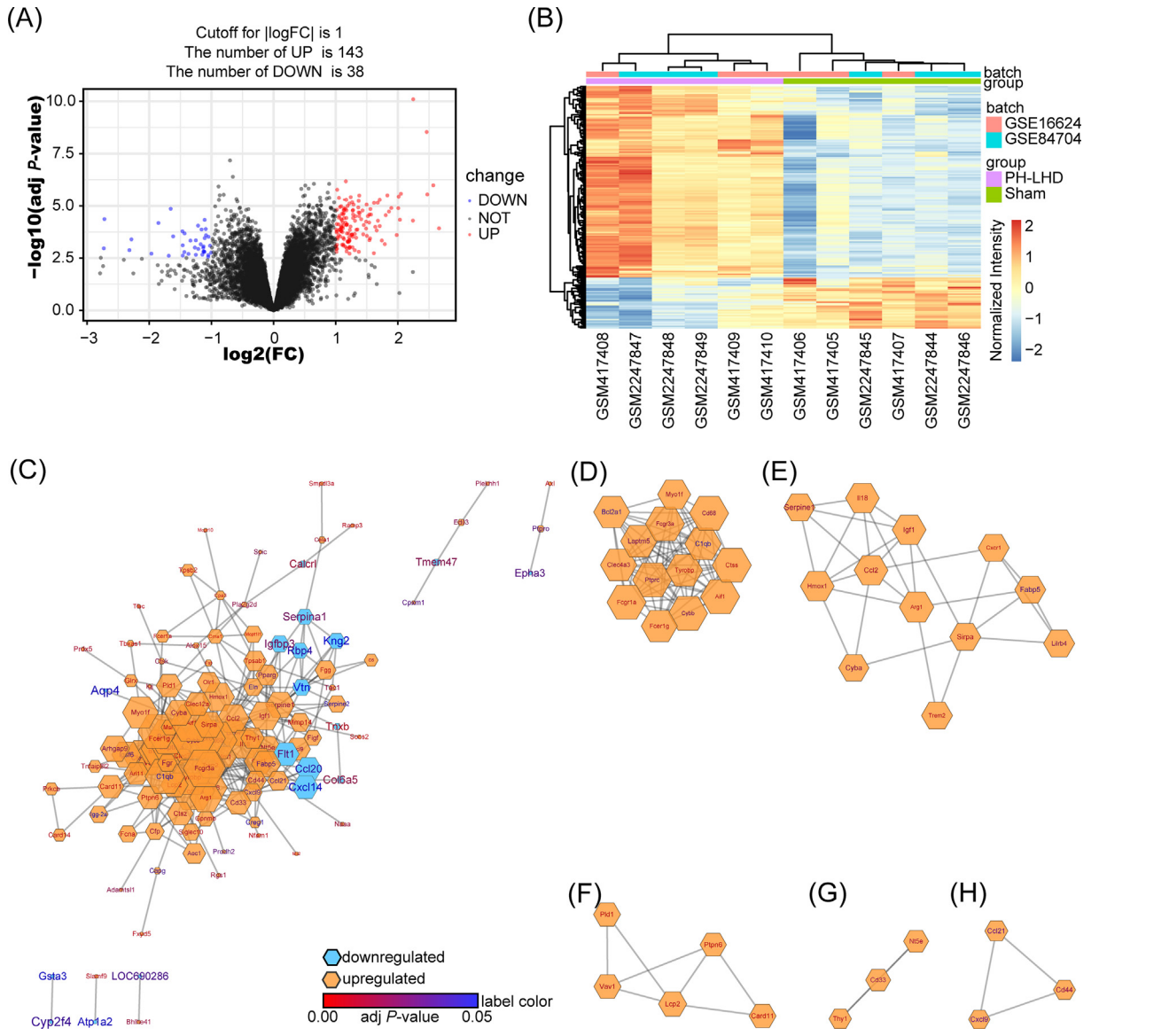

Fig. 1. Bioinformatic analysis. (A) The volcano plot of DEGs. The blue dots stand for downregulated DEGs, grey dots stand for non-differentially DEGs and red dots stand for upregulated DEGs. (B) Heatmap of DEGs. The gradual color change from orange to white to blue indicates the changing relative expression of DEGs from upregulation to downregulation. GSE, GEO series; FC, fold-change; adj.P.Val, adjusted P-value. (C-H) A PPI network of the DEGs that one probe corresponds to one gene (C) and five modules (D-H). Orange nodes represent up-regulated DEGs, while blue nodes represent down-regulated DEGs. The bigger size of nodes stands for a bigger node degree. The bigger of size label font indicates a bigger value of logFC. The gradual color of label from blue to red indicates the gradually decreased adj *P*-value of DEGs.

Taken together, inhibition of FABP5 improved cardiac function and attenuated PH-LHD caused pulmonary vascular remodeling and fibrosis.

FABP5 inhibition or knockdown downregulated TGF-β1-mediated expression of pro-fibrotic proteins in PAFs

To assess whether FABP5 mediates PH-LHD-induced pulmonary artery fibrosis in vitro, we used SBFI-26 to inhibit FABP5. While TGF-β1 stimulation increased profibrogenic proteins Col1 and α-SMA in PAFs, inhibition of FABP5 blocked TGF-β1-induced increases of these profibrogenic proteins (Fig. 4A). We next used siRNA to knock down FABP5 in PAFs (Fig. 4B). FABP5 siRNA blunted the fibrotic effect of TGF-β1, as shown by the immunofluorescence staining with α-SMA antibody (Fig. 4C) and attenuated of TGF-β1-induced increases of profibrogenic proteins (Fig. 4D). These results demonstrated that FABP5 plays a crucial role in regulating the fibrotic response in PAFs.

FABP5 induced PAF activation is mediated by wnt/β-catenin pathway

We investigated the role of wnt/β-catenin pathway in FABP5-mediated fibrotic response in PAFs and found that FABP5 siRNA treatment effectively inhibited the wnt/β-catenin activation in TGF-β1-treated PAFs, as demonstrated by the decreased p-GSK3β/GSK3β and PPARδ and increased p-β-catenin/β-catenin levels (Fig. 5A). Importantly, we used SKL2001 to activate wnt/β-catenin pathway, and found that SKL2001 application largely reversed the FABP5 siRNA-induced downregulation of Col1 and α-SMA in PAFs under TGF-β1 stimulation (Fig. 5B). These results collectively indicate that FABP5 is involved in pulmonary artery fibrosis partly via activating the wnt/β-catenin pathway.

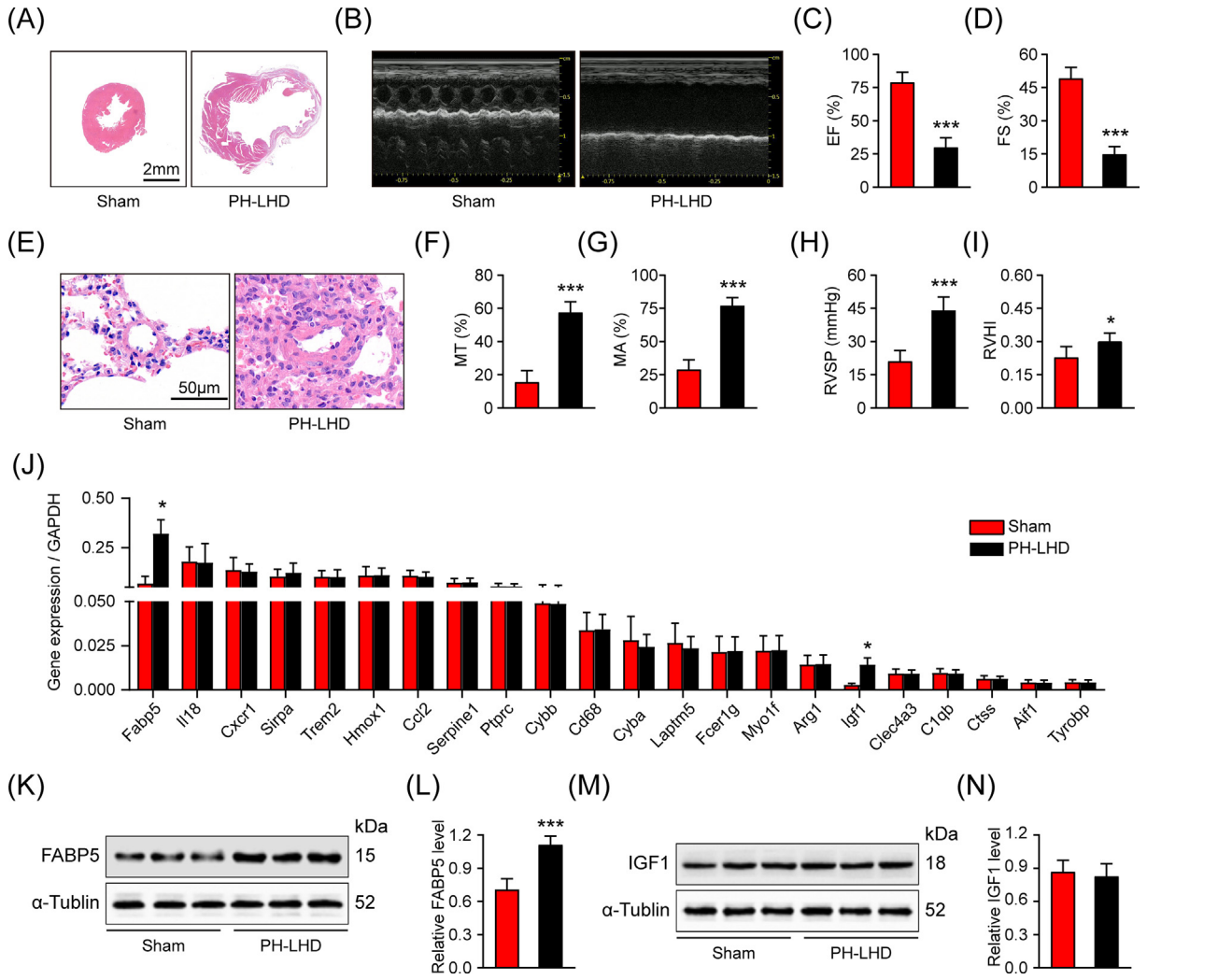

Fig. 2. FABP5 was identified as a potential target for PH-LHD treatment. (A) Representative HE staining of heart in sham/PH-LHD mice. (B-D) Representative M-mode images of echocardiography (B) and average data of EF (C) and FS (D) in sham/PH-LHD mice. n = 6, ***P < 0.001. (E-G) Representative HE staining of pulmonary arteries (E) showing MT% (F) and MA% (G) of pulmonary arteries in sham/PH-LHD mice. Scale bar = 50 μm. n = 60. ***P < 0.001. (H) Average data of RVSP in sham/PH-LHD mice. n = 6, ***P < 0.001. (I) Average data of RVHI in sham/PH-LHD mice. n = 6, *P < 0.05. (J) RT-qPCR results of 22 genes expression in sham/PH-LHD mice. (K-L) Western blot and average data showing FABP5 protein levels in sham/PH-LHD mice. n = 6, ***P < 0.001. (M-N) Western blot and average data showing IGF1 protein levels in sham/PH-LHD mice. n = 6.

Discussion

In this study, FABP5 was identified by bioinformatic analysis of two microarray datasets (GSE84704 and GSE16624) and validated using RT-qPCR and western blot in PH-LHD mice. In vivo FABP5 inhibition by SBFI-26 improved cardiac function and suppressed pulmonary artery remodeling in PH-LHD mice. In vitro study revealed that application of SBFI-26 and FABP5 siRNA blunted TGF-β1-induced fibrotic response in PAFs. Moreover, FABP5 activated wnt/β-catenin pathway, and wnt/β-catenin activation eliminated the anti-fibrotic effect of FABP5 knockdown. Therefore, the FABP5 could be an important potential target for PH-LHD. Thus, FABP5 and its regulated wnt/β-catenin pathway could be the therapeutic targets for PH-LHD.

PH occurs in LHD when left heart filling pressure passively elevated [4]. MI mouse model is the frequently used animal model of heart failure with secondary PH [23]. In this study, left heart failure post MI surgery was confirmed by histological staining with manifestation of the left ventricular dilation and left wall thinning (Fig. 2A) and by echocardiography manifested by significant reduction of left ventricular EF and FS% (Fig. 2B). It was proposed that the most important pathology of pH is pulmonary vascular remodelling [24]. In heart failure patients, the severity of pH correlated strongly with venous and arteriolar intimal thickening [25]. Our PH-LHD model recapitulates this feature by showing that MT% and MA% were significantly increased in pulmonary artery. Of all selected genes, FABP5 was identified as the only upregulated gene in this PH-LHD model. Therefore, FABP5 was expected to be a new intervention target in PH-LHD.

The fatty acid-binding proteins (FABPs) are lipid-chaperones which take part in various lipid-mediated biological processes [26]. As an import member of FABPs family, FABP5 is most abundantly expressed in epidermis, although it is also expressed in heart, lung, kidney, and other tissues [27]. To date, FABP5 has not been studied in the pulmonary artery diseases, although its associations with COPD and lung cancer have been reported. FABP5 was reported to be downregulated in human bronchial epithelial in cigarette smoker with COPD, and its expression was associated with regulation of anti-inflammation response in infectious lung diseases [28]. In addition, the enhanced expression of FABP5 in lung can promote the occurrence and metastasis of non-small cell lung cancer [29]. However, the role of FABP5 in PH-LHD pathogenesis remains poorly understood.

PPARβ/δ is the downstream effector of FABP5 [30]. After binding with fatty acids, FABP5 translocates from cytoplasmic to nuclear and then stimulates PPARβ/δ to activate the transcription of target

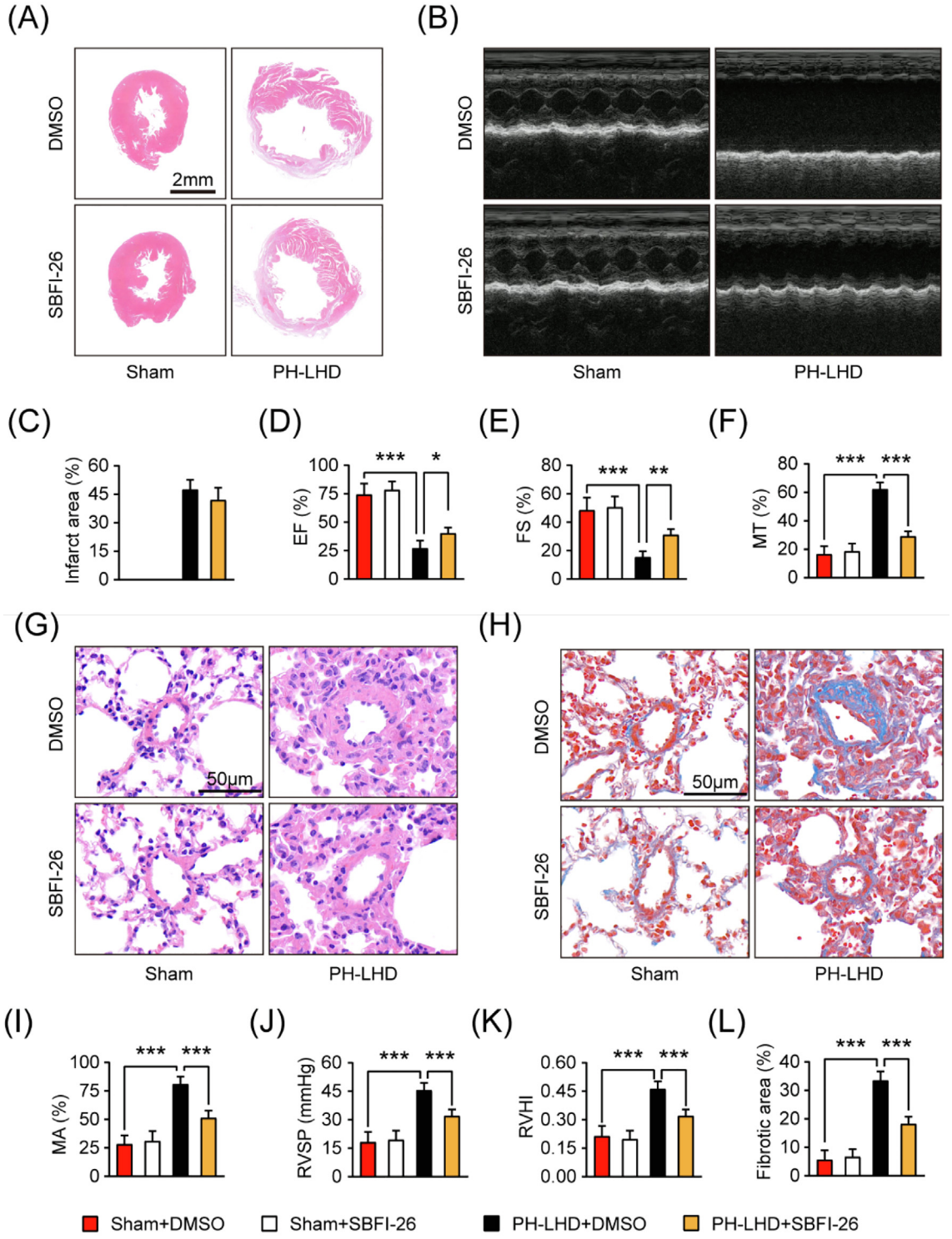

Fig. 3. Inhibition of FABP5 improved cardiac function and mitigated pulmonary vascular remodeling and fibrosis in PH-LHD. (A, C) Representative HE staining of heart (A) showing infarct size of heart (C) in sham/PH-LHD mice with/without SBFI-26 treatment. n = 6, Scale bar = 2 mm. (B, D, E) Representative M-mode images of echocardiography (B) and average data of EF (D) and FS (E) in sham/PH-LHD mice with/without SBFI-26 treatment. n = 6, $^{*}P < 0.05$, $^{**}P < 0.01$, $^{***}P < 0.001$. (F, G, I) Representative HE staining of pulmonary arteries (G) showing MT% (F) and MA% (I) of pulmonary arteries in sham/PH-LHD mice with/without SBFI-26 treatment. Scale bar = 50 μm. n = 6. $^{**}P < 0.01$, $^{***}P < 0.001$. (J) Average data of RVSP in sham/PH-LHD mice with/without SBFI-26 treatment. n = 6, $^{***}P < 0.001$. (K) Average data of RVHI in sham/PH-LHD mice with/without SBFI-26 treatment. n = 6, $^{***}P < 0.001$. (H, L) Representative masson trichrome staining (H) showing collagen deposition in the pulmonary arteries and their border zones (L) in sham/PH-LHD mice with/without SBFI-26 treatment. Scale bar = 50 μm. n = 6, $^{***}P < 0.001$.

genes [30]. It has been reported that PPARδ agonists reversed the ethanol-induced suppression of wnt/β-catenin pathway in mouse liver [31]. There is no study tested whether or how FABP5 regulates wnt/β-catenin pathway, although FABP5 was reported to be negatively regulated by wnt/β-catenin pathway [32]. The canonical wnt/β-catenin signalling pathway plays an important role in pulmonary vascular remodelling process. In congenital heart disease-related PH, wnt/β-catenin signalling was reported to be

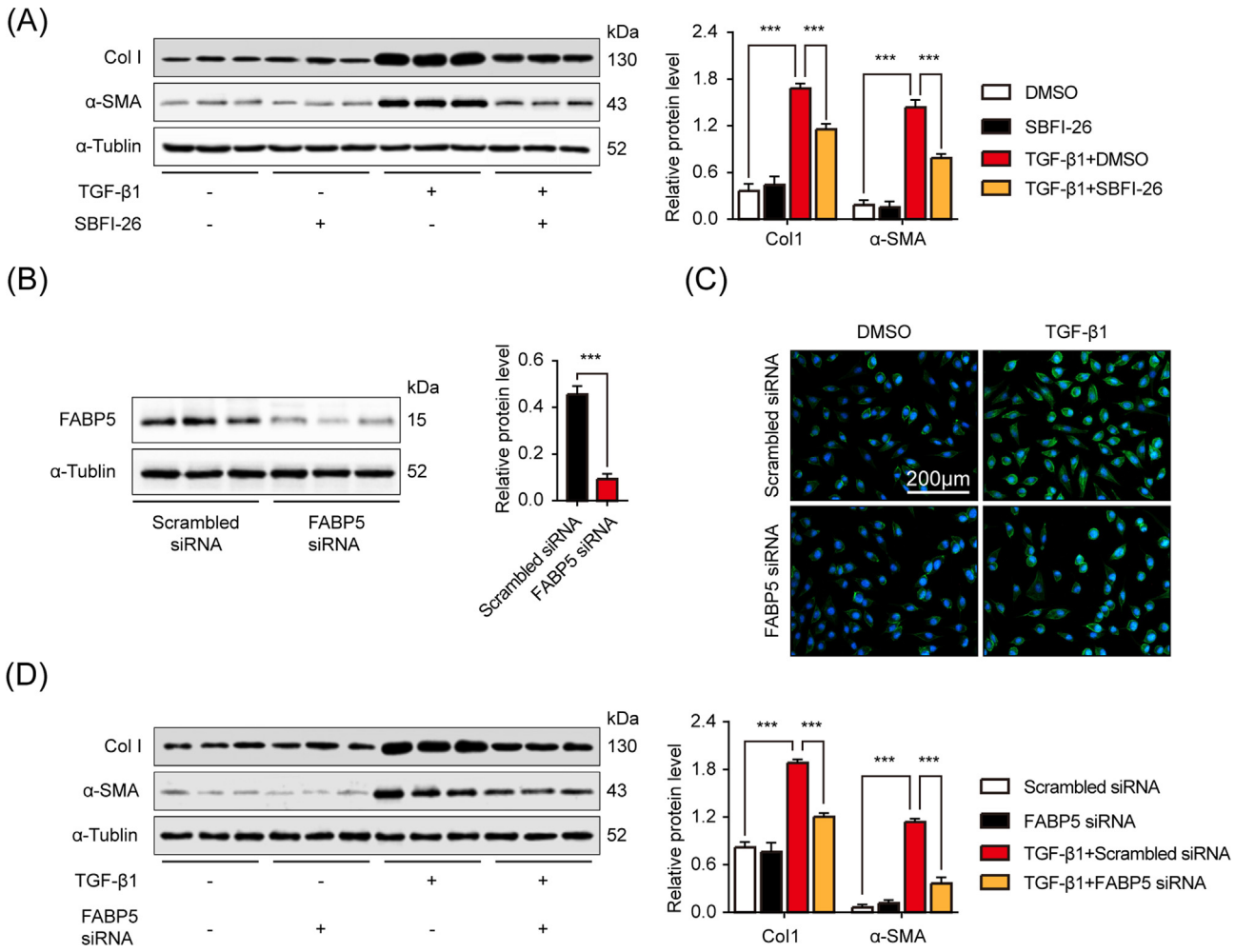

Fig. 4. Both inhibition of FABP5 and knockdown FABP5 downregulated TGF-β1-mediated expression of pro-fibrotic proteins in PAFs. (A) Western blot and average data showing Col1 and α-SMA protein levels in PAFs treated with/without SBFI-26 with/without TGF-β1 stimulation. n = 3, ***$P < 0.001$. (B) Western blot and average data showing FABP5 protein level in PAFs with/without FABP5 knockdown. n = 3, ***$P < 0.001$. (C) Immunofluorescence staining of α-SMA in PAFs with/without FABP5 knockdown treated with/without TGF-β1 stimulation. Scale bar = 200 μm. (D) Western blot and average data showing Col1 and α-SMA protein levels in PAFs with/without FABP5 knockdown treated with/without TGF-β1 stimulation. n = 3, ***$P < 0.001$.

significantly activated in pulmonary artery smooth muscle cells (PASMCs). The enhanced wnt/β-catenin signalling can promote aberrant proliferation of PASMCs and pulmonary vascular remodelling [33]. In the context of hyperoxia-induced lung injury, the expression and nuclear translocation of β-catenin were markedly increased, and both were closely associated with PH, as inhibition of wnt/β-catenin attenuated hyperoxia-induced lung injury and PH development [34]. Here, we reported that FABP5 induced pulmonary vascular remodelling in PH-LHD was largely mediated by wnt/β-catenin signalling.

Wnt/β-catenin pathway is highly conserved in evolution and involved in diverse processes, including balance of energy metabolism, embryonic development and cancer pathogenesis [35]. In the process of wnt/β-catenin pathway activation, cytoplasmic protein level of β-catenin functions as a switch. β-catenin at low level keeps wnt/β-catenin pathway from activation. But when wnt ligand binds to transmembrane receptors Frizzled and LRP-5/6 and forms a complex, it activates plasmosin Dishevelled. The activated Dishevelled suppresses the formation of the destruction complex (comprised of GSK-3β, APC and Axin), and then inhibits β-catenin phosphorylation, leading to a sharp reduction of β-catenin degradation mediated by ubiquitylation and proteasome [36]. The accumulated β-catenin transfers to the nucleus and binds to TCF (T cell factor)/LEF1 (lymphoid enhancer-binding factor 1) transcription factor family, regulating the expression of target genes [37]. Hence, the phosphorylation level of GSK-3β and β-catenin is the biomarker of the wnt/β-catenin pathway activation.

In this study, we found that FABP5 knockdown downregulated the phosphorylation level of GSK-3β and upregulated the phosphorylation level of β-catenin, resulting in inactivation of wnt/β-catenin pathway and elimination of the fibrotic response. Our data was consistent with the previous findings that activation of wnt/β-catenin pathway caused PH deterioration [22] and fibroblast activation [38]. For the first time, we demonstrate that FABP5 is the driving force.

On the other hand, our study found that FABP5 inhibition could improve cardiac function in this MI-induced heart failure model, which is inconsistent with findings from a pressure-overload heart failure model [39]. Gao et al recently reported decreased cardiac function in FABP5 knockout mice with transverse aortic constriction (TAC)-induced heart failure [39]. Discrepancy between the studies may derive from distinct types of mouse model. In our study, a severe heart failure model was constructed through permanent ligation of coronary LMA. This MI-induced heart failure model is characterized by the massive loss of cardiomyocytes and subsequent intensive inflammatory response. As a result of

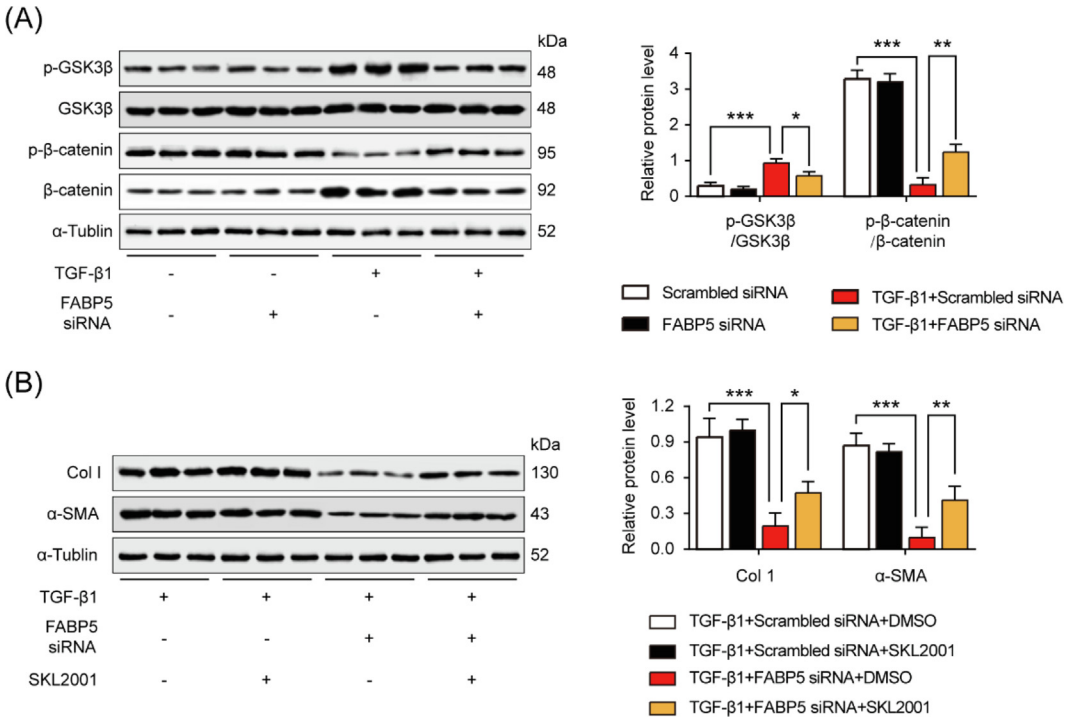

Fig. 5. FABP5 regulated PAF activation partly via activating wnt/β-catenin pathway. (A) Western blot and average data showing the protein levels of GSK3β, p-GSK3β, β-catenin and p-β-catenin in PAFs with/without FABP5 knockdown with/without TGF-β1 stimulation. n = 3, $^{*}P < 0.05$, $^{**}P < 0.01$, $^{***}P < 0.001$. (B) Western blot and average data showing the protein levels of profibrogenic proteins Col1 and α-SMA in TGF-β1 stimulated PAFs with/without FABP5 knockdown treated with/without wnt/β-catenin pathway agonist SKL2001. n = 3, $^{*}P < 0.05$, $^{**}P < 0.01$, $^{***}P < 0.001$.

FABP5 inhibition, the diminished PH will improve pulmonary perfusion and myocardial ischemia. These could explain the improved cardiac function in our ischemic mouse model in which disrupted pulmonary perfusion played essential roles in the development of cardiac dysfunction [40]. In contrast, Gao et al investigated the role of FABP5 in TAC-induced heart failure in the FABP5 knockout mice, where myocardial hypertrophy and mitochondrial dysfunction are the main pathology. In this setting, the myocardial deficiency of FABP5 could accelerate the mitochondrial dysfunction and therefore aggravate heart dysfunction [39]. Since FABP5 can regulate inflammation process, which is critical for heart failure progression after MI, FABP5 may also affect cardiac function through modulating inflammatory response in the setting of MI.

Conclusion

Collectively, this study demonstrates that FABP5 plays a crucial role in the development of PH-LHD by activating wnt/β-catenin signalling pathway. These findings point out FABP5 as a potential target for anti-PH-LHD therapy.

Compliance with Ethics Requirements

All Institutional and National Guidelines for the care and use of animals (fisheries) were followed.

All animal studies were conducted in accordance with the Animal Care and Use Committee Guide of Wuhan University, which conforms to the Guide for the Care and Use of Laboratory Animals of the National Institutes of Health (NIH publication no. 85-23, revised 1996).

Declaration of Competing Interest

The authors declare that they have no known competing financial interests or personal relationships that could have appeared to influence the work reported in this paper.

Acknowledgements

This work was supported by grants awarded to Yanggan Wang from the National Natural Science of China (NSFC, Grant Nos. 82070348, 81270304, 81873507 and 81420108004).

Appendix A. Supplementary material

Supplementary data to this article can be found online at https://doi.org/10.1016/j.jare.2021.11.011.

References

[1] Spiekerkoetter E, Kawut SM, de Jesus Perez VA. New and Emerging Therapies for Pulmonary Arterial Hypertension. Annu Rev Med 2019;70(1):45–59.
[2] Naeije R, D'Alto M. The Diagnostic Challenge of Group 2 Pulmonary Hypertension. Prog Cardiovasc Dis 2016;59(1):22–9.
[3] Do.e Z, Fukumoto Y, Takaki A, Tawara S, Ohashi J, Nakano M, et al. Evidence for Rho-kinase activation in patients with pulmonary arterial hypertension. Circ J 2009;73(9):1731–9.
[4] Guazzi M, Borlaug BA. Pulmonary hypertension due to left heart disease. Circulation 2012;126(8):975–90.
[5] Rosenkranz S. Pulmonary hypertension 2015: current definitions, terminology, and novel treatment options. Clin Res Cardiol 2015;104(3):197–207.
[6] McKillop IH, Girardi CA, Thompson KJ. Role of fatty acid binding proteins (FABPs) in cancer development and progression. Cell Signal 2019;62:109336. doi: https://doi.org/10.1016/j.cellsig.2019.06.001.
[7] Storch J, Corsico B. The emerging functions and mechanisms of mammalian fatty acid-binding proteins. Annu Rev Nutr 2008;28(1):73–95.

[8] Hotamisligil GS, Bernlohr DA. Metabolic functions of FABPs–mechanisms and therapeutic implications. Nat Rev Endocrinol 2015;11(10):592–605.
[9] Thumser AE, Moore JB, Plant NJ. Fatty acid binding proteins: tissue-specific functions in health and disease. Curr Opin Clin Nutr Metab Care 2014;17 (2):124–9.
[10] Ghelfi E, Karaaslan C, Berkelhamer S, Akar S, Kozakewich H, Cataltepe S. Fatty acid-binding proteins and peribronchial angiogenesis in bronchopulmonary dysplasia. Am J Respir Cell Mol Biol 2011;45(3):550–6.
[11] Guaita-Esteruelas S, Gumà J, Masana L, Borràs J. The peritumoural adipose tissue microenvironment and cancer. The roles of fatty acid binding protein 4 and fatty acid binding protein 5. Mol Cell Endocrinol 2018;462:107–18.
[12] Cussac L-A, Cardouat G, Tiruchellvam Pillai N, Campagnac M, Robillard P, Montillaud A, et al. TRPV4 channel mediates adventitial fibroblast activation and adventitial remodeling in pulmonary hypertension. Am J Physiol Lung Cell Mol Physiol 2020;318(1):L135–46.
[13] JIANG Y-L, DAI A-G, LI Q-F, HU R-C. Transforming growth factor-beta1 induces transdifferentiation of fibroblasts into myofibroblasts in hypoxic pulmonary vascular remodeling. Acta Biochim Biophys Sin (Shanghai) 2006;38(1):29–36.
[14] Song J, Zhang H, Wang Z, Xu W, Zhong Li, Cao J, et al. The Role of FABP5 in Radiation-Induced Human Skin Fibrosis. Radiat Res 2018;189(2):177. doi: https://doi.org/10.1667/RR14901.110.1667/RR14901.1.s1.
[15] Gautier L, Cope L, Bolstad BM, Irizarry RA. affy–analysis of Affymetrix GeneChip data at the probe level. Bioinformatics 2004;20(3):307–15.
[16] Ritchie ME, Phipson B, Wu D, Hu Y, Law CW, Shi W, et al. limma powers differential expression analyses for RNA-sequencing and microarray studies. Nucleic Acids Res 2015;43:e47.
[17] Szklarczyk D, Franceschini A, Wyder S, Forslund K, Heller D, Huerta-Cepas J. STRING v10: protein-protein interaction networks, integrated over the tree of life. Nucleic Acids Res 2015;43:D447–52.
[18] Shannon P, Markiel A, Ozier O, Baliga NS, Wang JT, Ramage D. Cytoscape: a software environment for integrated models of biomolecular interaction networks. Genome Res 2003;13:2496–504.
[19] Bader GD, Hogue CWV. An automated method for finding molecular complexes in large protein interaction networks. BMC Bioinformatics 2003;4 (2). doi: https://doi.org/10.1186/1471-2105-4-2.
[20] Al-Jameel W, Gou X, Forootan SS, Al Fayi MS, Rudland PS, Forootan FS, et al. Inhibitor SBFI26 suppresses the malignant progression of castration-resistant PC3-M cells by competitively binding to oncogenic FABP5. Oncotarget 2017;8:31041–56.
[21] Aliotta JM, Pereira M, Wen S, Dooner MS, Del Tatto M, Papa E, et al. Exosomes induce and reverse monocrotaline-induced pulmonary hypertension in mice. Cardiovasc Res 2016;110:319–30.
[22] Mair KM, MacLean MR, Morecroft I, Dempsie Y, Palmer TM. Novel interactions between the 5-HT transporter, 5-HT1B receptors and Rho kinase in vivo and in pulmonary fibroblasts. Br J Pharmacol 2008;155:606–16.
[23] Jasmin J-F, Mercier I, Hnasko R, Cheung MWC, Tanowitz HB, Dupuis J, et al. Lung remodeling and pulmonary hypertension after myocardial infarction: pathogenic role of reduced caveolin expression. Cardiovasc Res 2004;63:747–55.
[24] Jeffery TK, Wanstall JC. Pulmonary vascular remodeling: a target for therapeutic intervention in pulmonary hypertension. Pharmacol Therapeutics 2001;92.
[25] Fayyaz AU, Edwards WD, Maleszewski JJ, Konik EA, DuBrock HM, Borlaug BA, et al. Global Pulmonary Vascular Remodeling in Pulmonary Hypertension Associated With Heart Failure and Preserved or Reduced Ejection Fraction. Circulation 2018;137(17):1796–810.
[26] Nguyen HC, Qadura M, Singh KK. Role of the Fatty Acid Binding Proteins in Cardiovascular Diseases: A Systematic Review. J Clin Med 2020;9(11):3390. doi: https://doi.org/10.3390/jcm9113390.
[27] Makowski L, Hotamisligil GS. The role of fatty acid binding proteins in metabolic syndrome and atherosclerosis. Curr Opin Lipidol 2005;16:543–8.
[28] Rao D, Perraud A-L, Schmitz C, Gally F, Kalinichenko VV. Cigarette smoke inhibits LPS-induced FABP5 expression by preventing c-Jun binding to the FABP5 promoter. PLoS ONE 2017;12(5):e0178021. doi: https://doi.org/10.1371/journal.pone.017802110.1371/journal.pone.0178021.g00110.1371/journal.pone.0178021.g00210.1371/journal.pone.0178021.g00310.1371/journal.pone.0178021.g004.
[29] Ni K, Wang D, Xu H, Mei F, Wu C, Liu Z, et al. miR-21 promotes non-small cell lung cancer cells growth by regulating fatty acid metabolism. Cancer Cell Int 2019;19(1). doi: https://doi.org/10.1186/s12935-019-0941-8.
[30] Yu S, Levi L, Casadesus G, Kunos G, Noy N. Fatty acid-binding protein 5 (FABP5) regulates cognitive function both by decreasing anandamide levels and by activating the nuclear receptor peroxisome proliferator-activated receptor β/δ (PPARβ/δ) in the brain. J Biol Chem 2014;289(18):12748–58.
[31] Xu CQ, de la Monte SM, Tong M, Huang C-K, Kim M. Chronic Ethanol-Induced Impairment of Wnt/β-Catenin Signaling is Attenuated by PPAR-δ Agonist. Alcohol Clin Exp Res 2015;39(6):969–79.
[32] Collins CA, Watt FM. Dynamic regulation of retinoic acid-binding proteins in developing, adult and neoplastic skin reveals roles for beta-catenin and Notch signalling. Dev Biol 2008;324:55–67.
[33] Zhou J-J, Li H, Qian Y-L, Quan R-L, Chen X-x, Li Li, et al. Nestin represents a potential marker of pulmonary vascular remodeling in pulmonary arterial hypertension associated with congenital heart disease. J Mol Cell Cardiol 2020;149:41–53.
[34] Alapati D, Rong M, Chen S, Lin C, Li Y, Wu S. Inhibition of LRP5/6-mediated Wnt/β-catenin signaling by Mesd attenuates hyperoxia-induced pulmonary hypertension in neonatal rats. Pediatr Res 2013;73(6):719–25.
[35] Rosenbluh J, Wang X, Hahn WC. Genomic insights into WNT/β-catenin signaling. Trends Pharmacol Sci 2014;35(2):103–9.
[36] Clevers H, Nusse R. Wnt/β-catenin signaling and disease. Cell 2012;149 (6):1192–205.
[37] Baarsma HA, Königshoff M. WNT signalling in chronic lung diseases. Thorax 2017;72:746–59.
[38] Xiang F-L, Fang M, Yutzey KE. Loss of β-catenin in resident cardiac fibroblasts attenuates fibrosis induced by pressure overload in mice. Nat Commun 2017;8:712.
[39] Gao S, Li G, Shao Y, Wei Z, Huang S, Qi F, et al. FABP5 Deficiency Impairs Mitochondrial Function and Aggravates Pathological Cardiac Remodeling and Dysfunction. Cardiovasc Toxicol 2021;21(8):619–29.
[40] Bacmeister L, Schwarzl M, Warnke S, Stoffers B, Blankenberg S, Westermann D, et al. Inflammation and fibrosis in murine models of heart failure. Basic Res Cardiol 2019;114(3). doi: https://doi.org/10.1007/s00395-019-0722-5.